

CAILA: Concept-Aware Intra-Layer Adapters for Compositional Zero-Shot Learning

Zhaoheng Zheng Haidong Zhu Ram Nevatia
Viterbi School of Engineering
University of Southern California
{zhaoheng.zheng, haidongz, nevatia}@usc.edu

Abstract

Compositionality, the ability to combine existing concepts and generalize towards novel compositions, is a key functionality for intelligent entities. Here, we study the problem of Compositional Zero-Shot Learning (CZSL), which aims at recognizing novel attribute-object compositions. Recent approaches build their systems on top of large-scale Vision-Language Pre-trained (VLP) models, e.g. CLIP, and observe significant improvements. However, these methods treat CLIP as a black box and focus on pre- and post-CLIP operations. Here, we propose to dive deep into the architecture and insert adapters, a parameter-efficient technique proven to be effective among large language models, to each CLIP encoder layer. We further equip adapters with concept awareness so that concept-specific features of “object”, “attribute” and “composition” can be extracted. We name our method **CAILA**, **Concept-Aware Intra-Layer Adapters**. Quantitative evaluations performed on three popular CZSL datasets, MIT-States, C-GQA, and UT-Zappos, reveal that CAILA achieves double-digit relative improvements against the current state-of-the-art on all benchmarks.

1. Introduction

The ability to combine existing concepts and generalize to novel compositions, also known as compositionality, is a key functionality for an intelligent entity. It should be able to perceive individual primitives from known concepts and combine them into novel compositions. It is natural for a human to decompose individual primitives (*large*, *old*, *castle*, *bear*) from known concepts (*large bear*, *old castle*) and gain knowledge of novel concepts (*large castle*, *old bear*) by composing individual primitives. Researchers have formulated the problem as Compositional Zero-Shot Learning (CZSL) [25], where models are expected to generalize the knowledge learned from a set of seen attribute-

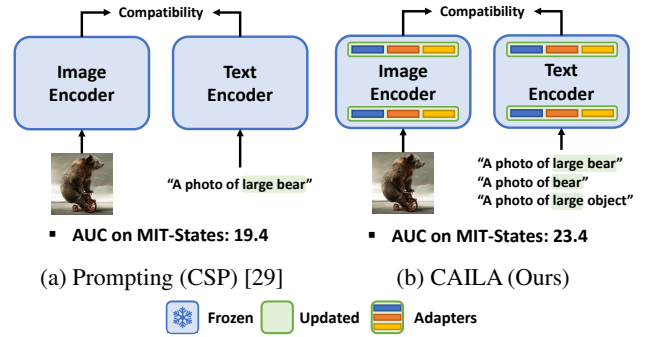


Figure 1: Illustrations of CAILA and previous CLIP-based baselines. Compared with soft prompting (a), CAILA (b) has adapters integrated into both CLIP encoders and thus better transfers the knowledge from CLIP to CZSL, resulting in significant performance boosts. Prompts highlighted in green are set to be learnable parameters.

object pairs and recognize novel compositions. Traditional methods[26, 27] suffer from biases in the training data while recent CLIP-based methods [29, 4] treat CLIP as a frozen encoder and do not optimize its knowledge for CZSL; we investigate adding parameter-efficient [7] components to better leverage knowledge from CLIP for CZSL.

In CZSL, all individual primitives are seen as parts of a composition during training but only a fraction of the potential compositional pairs is seen. The most common generalized CZSL benchmark [32] requires a model to recognize unseen compositions while maintaining the ability to recognize compositions in the training set. The challenge is to learn from the training set while avoiding biases towards the seen compositions. Thus, learning general representations that are composition-independent is critical for learning a feasible CZSL model. Previous methods [21, 1, 20, 24, 36, 32, 41, 44, 28, 27, 25, 40, 26] build their systems with pre-trained image encoders, e.g. ResNet [6] and independent word embeddings like GloVe [31] are limited by the amount of training data and so they are prone to

the known composition bias.

Recent advances in large-scale Vision-Language Pre-training (VLP) models [33, 19, 11] have greatly expanded the number of image-text pairs that a model can learn from. Therefore, VLP models have strong generalization ability and are suitable for CZSL tasks. However, prompt-tuning methods [29, 48, 49] only learn trainable prompts, while CLIP-Adapter [4] only adds external modules at the end of CLIP. Neither of them touches the CLIP encoder and all leave CLIP as a frozen black box model. Nayak *et al.* [29] show that fully fine-tuning CLIP leads to poor performance on CZSL due to overfitting to the training data. We argue that it is challenging to effectively leverage the knowledge from CLIP without modifying its internal structure. Therefore, a feasible CLIP-based CZSL should: i) be capable of extracting concept-specific features related to both compositions and individual primitives; ii) have task-specific architectural designs to accommodate the needs of CZSL.

As discussed in [7], on NLP benchmarks, a frozen transformer backbone with trainable adapters can achieve comparable performance with the fully fine-tuned model, while only $\sim 5\%$ parameters are trained. These features make adapters a good candidate for CZSL as they can transfer the knowledge from CLIP while avoiding strong training biases. Furthermore, as adapters are light-weight modules, it is practical to leverage multiple adapters for different concepts. Thus, in this paper, we propose **CAILA**, **C**oncept-**A**ware **I**ntra-**L**ayer **A**dapters, which are integrated inside the CLIP model, and improve model generalizability.

Given a pair of image and text, our model extract features from two separate encoders and compute the compatibility score between them. Illustrations in Fig. 1 reveal two major distinctions between CAILA and an earlier CLIP-based baseline: CAILA has a group of adapters integrated into each layer of both encoders; each group has concept-specific components to extract knowledge that corresponds to particular concepts including attributes, objects and compositions. To fuse features extracted by various concept-aware adapters, we propose the **Mixture-of-Adapters (MoA)** mechanism for both vision and language encoder. As CAILA can extract concept-specific features, we propose **Primitive Concept Shift**, which creates additional vision embeddings by combining the attribute feature from one image and the object feature from the other.

We evaluate our approach on three popular CZSL datasets: MIT-States [10], C-GQA [26] and UT-Zappos [45, 46], under both closed world and open world settings. Our experiments demonstrate that, in both scenarios, our model outperforms the state-of-the-arts over all three existing benchmarks following the generalized evaluation protocol [32], by significant margins.

To summarize, our contributions are as follows: (i) We open up the black box of CLIP and insert adapters to lay-

ers of image and text encoders to balance model capacity and training bias robustness; (ii) we fuse the knowledge from concept-aware adapters through the Mixture-of-Adapter (MoA) mechanism to further improve the generalizability; (iii) we perform concept shift to exploit the power of CAILA and enrich the training data; (iv) we conduct extensive experiments in exploring the optimal setup for CAILA on CZSL. Quantitative experiments show that our model outperforms the SOTA by significant margins in both closed world and open world, on all three benchmarks.

2. Related Works

Zero-Shot Learning (ZSL). Unlike conventional fully-supervised learning, ZSL requires models to learn from side information without observing any visual training samples [17]. The side information comes from multiple non-visual resources such as attributes [17], word embeddings [39, 37], and text descriptions [34]. Notably, Zhang *et al.* [47] propose to learn a deep embedding model bridging the seen and the unseen, while [2, 43, 50] investigate generative models that produce features for novel categories. Moreover, [39, 12] integrate Graph Convolution Networks (GCN) [16] to better generalize over unseen categories.

Compositional Zero-Shot Learning (CZSL). Previous CZSL approaches are built with pre-trained image encoders, *e.g.* ResNet and separate word embeddings, *e.g.* GloVe [31]. More specifically, Li *et al.* [21] investigate the symmetrical property between objects and attributes, while Atzmon *et al.* [1] study the causal influence between the two. Moreover, Li *et al.* [20] construct a Siamese network with contrastive learning to learn better object/attribute prototypes. On the other hand, joint representations of compositions can be leveraged in multiple ways. [32] utilizes joint embeddings to control gating functions for the modular network, while [41, 44, 28, 27] treat them as categorical centers in the joint latent space. Furthermore, some approaches [25, 40, 26, 35, 24] directly take compositional embeddings as classifier weights, while OADis [36] disentangles attributes and objects in the visual space.

Parameter-Efficient Tuning. Recent research on large scale pre-training models [33, 11, 8, 19, 5] has achieved superior performance on various downstream tasks, compared with regular approaches. Though various works [7, 38, 13] show that tuning adapters [7] on the language side yields comparable results with fully fine-tuned variants, parameter-efficient tuning on image encoders are yet to be studied. For CZSL, a few models [49, 29] leverage the knowledge of CLIP through prompt tuning [18], while Gao *et al.* [4] attach a post-processor to CLIP for knowledge transfer. Though these methods show strong performance on CZSL against regular models, they treat the CLIP model as a black box and keep it completely frozen. In CAILA, we open up the CLIP black box by integrating intra-layer

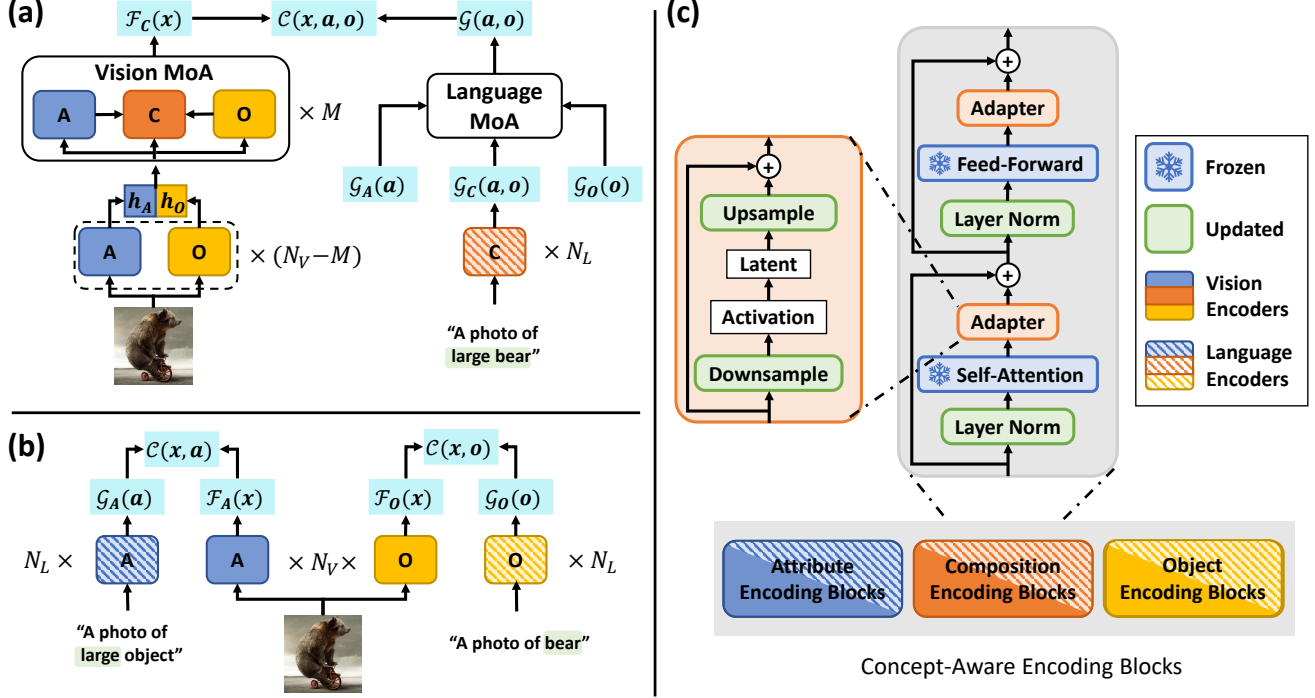


Figure 2: An overview of CAILA: (a) The main composition compatibility estimation pipeline; (b) Auxiliary sub-tasks on primitive compatibility during training; (c) The structure of CAILA layers. Our model extracts concept-specific features by learning different adapters and fuses them through the Mixture-of-Adapters (MoA) mechanism. Note that for each layer of encoders in (a) and (b), the weights of encoding blocks of the same concept are shared. N_V , N_L and M indicate depth.

adapters to both image and text encoders.

3. Approach

The problem of CZSL can be formulated as follows. We denote the training set by $\mathcal{T} = \{(x, y) | x \in \mathcal{X}, y \in \mathcal{Y}_s\}$, where \mathcal{X} contains images represented in the RGB color space and \mathcal{Y}_s is a set of seen composition labels which are available during the training phase. Each label $y = (a, o)$ is a pair of attribute $a \in \mathcal{A}$ and object category $o \in \mathcal{O}$. When testing, CZSL expects models to predict a set of unseen compositions \mathcal{Y}_u that is mutually exclusive with training labels \mathcal{Y}_s : $\mathcal{Y}_s \cup \mathcal{Y}_u = \emptyset$. Note that \mathcal{Y}_s and \mathcal{Y}_u share the same set of \mathcal{A}, \mathcal{O} , while CZSL assumes that each $a \in \mathcal{A}$ or $o \in \mathcal{O}$ exists in the training set and only the composition $(a, o) \in \mathcal{Y}_u$ is novel. Following [32, 42, 26], we focus on generalized CZSL, where the test set contains both seen and unseen labels, formally denoted by $\mathcal{Y}_{test} = \mathcal{Y}_s \cup \mathcal{Y}_u$.

Most recent works [26, 32, 1] study the generalized CZSL problem under the *closed world* setting, where \mathcal{Y}_{test} is a subset of the complete composition set $\mathcal{Y} : \mathcal{A} \times \mathcal{O}$. The *closed world* setting assumes that \mathcal{Y}_u are known during testing and thus greatly reduce the size of the search space. On the contrary, Mancini *et al.* [23] argue that such constraint should not be applied to the search space and in-

troduce the *open world* setting, where models are required to search over the complete set of compositions, formally $\mathcal{Y}_s \cup \mathcal{Y}_u = \mathcal{Y}$. In this paper, we investigate the problem in both *closed world* and *open world*.

3.1. Compatibility Estimation Pipeline

As different attributes can lead to significant appearance shifts even inside the same object category, performing attribute and object predictions separately may be ineffective. Hence, we model attribute-object compositions jointly and learn a combined estimation function to measure the compatibility of input image x and query composition (a, o) . In addition, we let the model estimate attribute and object compatibilities as auxiliary sub-tasks during training.

The estimation of composition compatibility is represented as $\mathcal{C}(x, a, o) : \mathcal{X} \times \mathcal{A} \times \mathcal{O} \rightarrow \mathbb{R}$. It contains two components: The image feature extractor $F_C : \mathbb{R}^{H \times W \times 3} \rightarrow \mathbb{R}^d$ and the text embedding generator $G : \mathcal{A} \times \mathcal{O} \rightarrow \mathbb{R}^d$. Note that d denotes the number of channels that each representation has. Given an image x and a composition (a, o) , the compatibility score is defined as the dot product of $F_C(x)$ and $G(a, o)$, formally

$$\mathcal{C}(x, a, o) = F_C(x) \cdot G(a, o). \quad (1)$$

Furthermore, as CZSL requires models to recognize novel pairs composed of known attributes and objects, it is important for a model to possess the capability of primitive feature extraction that is disentangled with training compositions. Thus, we make our model extract features corresponding to primitives and estimate the compatibility between vision features and text representations during training. Similar to Eqn. 1, we have

$$\mathcal{C}(x, a) = \mathcal{F}_A(x) \cdot \mathcal{G}_A(a), \mathcal{C}(x, o) = \mathcal{F}_O(x) \cdot \mathcal{G}_O(o). \quad (2)$$

All three compatibility scores contribute independently to the loss function in Eqn. 7, while $\mathcal{C}(x, a, o)$ is leveraged during inference. More specifically, our framework learns separate representations through CAILA discussed in Sec. 3.2 and conducts knowledge fusion through Mixture-of-Adapters (MoA), which will be covered in Sec. 3.3.

Following [33], we create a prompt template similar to "a photo of [CLASS]" for each compatibility estimation sub-task. For composition compatibility, we feed the text encoder with "a photo of [ATTRIBUTE] [OBJECT]"; We use "a photo of [ATTRIBUTE] object" and "a photo of [OBJECT]" for attribute and object compatibilities, respectively. Similar to [29], we only make [CLASS] prompts trainable. For both encoders \mathcal{F} and \mathcal{G} , we take the output hidden state of the [CLS] token as the representation.

3.2. Concept-Aware Intra-Layer Adapters

Though CLIP-based CZSL approaches [29, 4, 49] have achieved significant improvements compared with earlier methods [25, 26, 23, 32, 29], the CLIP encoder is considered as a black box and no modifications are made to improve its generalizability. Thus, we propose to improve CLIP-based CZSL models in both directions with CAILA, Concept-Aware Intra-Layer Adapters.

As shown in Fig. 2 (a)(b), we take the CLIP image encoder as \mathcal{F} and the text encoder as \mathcal{G} , while adding concept awareness to both encoders when estimating compatibilities of different concepts. Fig. 2 (c) demonstrates how adapters are integrated into a regular transformer encoding block. For each encoding block, we add adapters behind the frozen self-attention layer and the feed-forward network. More specifically, given the input hidden state \mathbf{h} of an adapter, we compute the latent feature \mathbf{z} by the downsampling operator f_{Down} , followed by the activation function σ . The output \mathbf{h}' of an adapter is obtained by upscaling \mathbf{z} and summing it with \mathbf{h} through the skip connection. Formally, we have

$$\mathbf{z} = \sigma(f_{Down}(\mathbf{h})), \quad \mathbf{h}' = f_{Up}(\mathbf{z}) + \mathbf{h}, \quad (3)$$

where both f_{Down} and f_{Up} are fully-connected layers.

To extract concept-specific features, at each depth level, we create three encoding blocks corresponding to attribute,

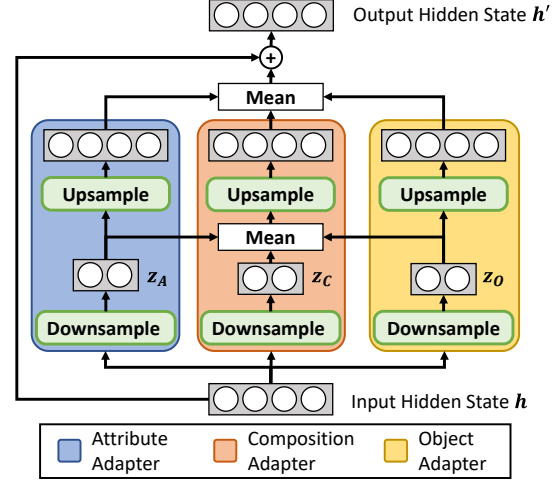


Figure 3: Details of our vision Mixture-of-Adapter. Latent features of each adapter, \mathbf{z}_A , \mathbf{z}_O , \mathbf{z}_C , are mixed, and further processed by the upsampling function to generate \mathbf{h}'_C . \mathbf{h}'_C is joined with \mathbf{h}'_A , \mathbf{h}'_O and input feature \mathbf{h} for output.

object, and composition, respectively. As in Fig. 2(c), encoding blocks of at the same level share the same weights except for the adapter layers. Inputs from both modalities are processed by encoders equipped with different types of encoding blocks and features related to each of the three concepts are produced. During training, vision-language compatibility scores for “attribute”, “object” and “compositions” are estimated. More specifically, vision encoding blocks of attributes in Fig. 2(a) and (b) for compositional compatibility and primitive compatibility, share the same weight; So are vision encoding blocks of objects.

3.3. MoA: Mixture of Adapters

To aggregate the knowledge extracted by adapters corresponding to attributes, objects, and compositions, we propose Mixture-of-Adapters mechanisms for both the vision side and language side of the encoder.

On the vision side, we perform a two-stage feature extraction. As shown in Fig. 2 (a), for the first $N_V - M$ layers, we extract features related to the attribute (\mathbf{h}_A) and the object (\mathbf{h}_O) through corresponding encoding blocks, which are further concatenated and processed by the trailing M ternary MoA layers. An example of the vision MoA layer is shown in Fig. 3. Given the hidden state \mathbf{h} , we first extract latent features \mathbf{z}_A , \mathbf{z}_O and \mathbf{z}_C from the adapters. We then combine all three latent features and create \mathbf{z}'_C , followed by f_{Up} , mapping it to \mathbf{h}'_C :

$$\mathbf{z}'_C = \text{Avg}[\mathbf{z}_A, \mathbf{z}_O, \mathbf{z}_C], \quad \mathbf{h}'_C = f_{Up}(\mathbf{z}'_C). \quad (4)$$

We further combine \mathbf{h}'_C with outputs of attribute and object

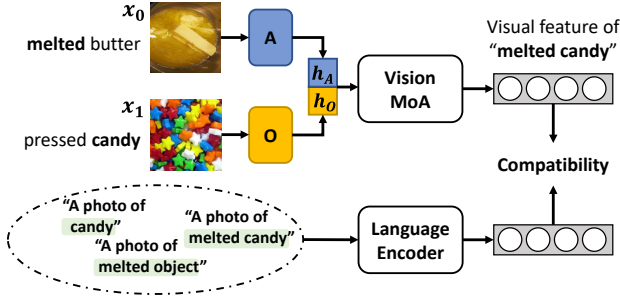


Figure 4: Illustrations of concept shift. We perform concept shift by combining the attribute (**melted**) feature from one image with the object (**candy**) feature to create an additional composition (**melted candy**) feature. Newly generated features are shuffled with regular samples during training.

adapters, h'_A and h'_O , to create the output:

$$h' = \text{Avg}[h'_A, h'_O, h'_C] + h. \quad (5)$$

The output of the last mixture layer is L2-normalized and adopted as $\mathcal{F}_C(x)$ for compatibility estimation.

Unlike the vision side, where attributes and objects are directly entangled within the same input image. On the language side, we can create disentangled language inputs through different prompt templates for attributes and objects separately. Thus, we adopt a simple mixture strategy for language adapters. We compute the compositional embedding through N_L encoding blocks for the composition and combine it with primitive language embeddings:

$$\mathcal{G}(a, o) = \text{Avg}[\mathcal{G}_A(a), \mathcal{G}_O(o), \mathcal{G}_C(a, o)]. \quad (6)$$

3.4. Primitive Concept Shift on Image Embeddings

Due to the limited diversity of training data, current CZSL models often suffer from training biases. As discussed in Sec. 3.3, in addition to the composition-related feature, CAILA extracts attribute- and object-oriented features during the first stage of \mathcal{F}_C . That motivates us to leverage these primitive-specific features to create additional embeddings for certain compositions. As it leads to changes in labels of original images, e.g. from melted butter to melted candy, we call it *primitive concept shift*.

Fig. 4 demonstrates the process of concept shift: Given one sample x_0 of melted butter and one sample x_1 of pressed candy, we create a new sample of melted candy in the feature space, by combining the attribute-oriented feature h_A of x_0 and the object-oriented feature h_O of x_1 . The newly combined feature is further processed by vision MoA layers described in Sec. 3.3, leading to an embedding representing melted candy. Such change can be viewed as an “object shift” from melted butter or an “attribute shift” from pressed candy. Thus, we

Dataset	Attr.	Obj.	Train Seen	Seen	Val Unseen	Test Seen	Test Unseen
MIT-States [10]	115	245	1k	300	300 (27k)	400	400 (27k)
C-GQA [26]	453	870	7k	1k	1k (387k)	1k	1k (387k)
UT-Zappos [45]	16	12	83	15	15 (109)	18	18 (109)

Table 1: Statistics of datasets for CZSL. The number in brackets is the size of unseen search space in *open world* for each dataset.

name this process “primitive concept shift”. In practice, we randomly pick a proportion of samples for shifting and ensure that the new label after shifting still lies in the training set. We discuss the effectiveness of the shifting in Sec. 4.3.

Although there are previous explorations [20, 41] in generating novel features in the latent space, our method is essentially novel from two aspects: i) Wei *et al.* [41] generate features directly from word embeddings, while our method leverages disentangled vision features that have richer and more diverse knowledge; ii) Li *et al.* [20] uses generated features to augment primitive vision encoders, while ours augments the entire model through CAILA for both compositions and individual primitives.

3.5. Training and Testing

Objective. We optimize our model with a main loss on attribute-object compositions and auxiliary losses on attributes and objects. As our model only has access to seen compositions Y_s , we create our training objective upon Y_s and ignore other compositions during training. More specifically, given an image x , we compute the compatibility score $\mathcal{C}(x, a, o)$, $\mathcal{C}(x, a)$ and $\mathcal{C}(x, o)$ for all $(a, o) \in Y_s$. We then jointly optimize \mathcal{F} and \mathcal{G} by the cross-entropy loss with temperature:

$$\mathcal{L} = \frac{-1}{|\mathcal{T}|} \sum_i \left\{ \log \frac{e^{[\mathcal{C}(x_i, a_i, o_i)/\tau_C]}}{\sum_j e^{[\mathcal{C}(x_i, a_j, o_j)/\tau_C]}} + \log \frac{e^{[\mathcal{C}(x_i, a_i)/\tau_A]}}{\sum_j e^{[\mathcal{C}(x_i, a_j)/\tau_A]}} + \log \frac{e^{[\mathcal{C}(x_i, o_i)/\tau_O]}}{\sum_j e^{[\mathcal{C}(x_i, o_j)/\tau_O]}} \right\}. \quad (7)$$

Intuitively, the cross-entropy loss will force the model to produce a higher compatibility score when (x, a, o) matches and lower the score when a non-label composition occurs.

Inference. The generalized CZSL task requires models to perform recognition over a joint set of seen and unseen compositions. Thus, for each test sample x , we estimate the compatibility score between x and every candidate (a, o) inside the search space $\mathcal{Y}_s \cup \mathcal{Y}_u$. We predict the image x as the composition that has the highest compatibility score:

$$\hat{y} = \arg \max_{(a, o) \in \mathcal{Y}_s \cup \mathcal{Y}_u} \mathcal{C}(x, a, o) \quad (8)$$

We apply the prediction protocol to all benchmarks.

	Closed World Model	● MIT-States				● C-GQA				● UT-Zappos			
		AUC (↑)	HM (↑)	S (↑)	U (↑)	AUC (↑)	HM (↑)	S (↑)	U (↑)	AUC (↑)	HM (↑)	S (↑)	U (↑)
Without CLIP	CompCos [23]	4.5	16.4	25.3	24.6	2.6	12.4	28.1	11.2	28.7	43.1	59.8	62.5
	ProtoProp [35]	-	-	-	-	3.7	15.1	26.4	18.1	34.7	50.2	62.1	65.7
	OADis [36]	5.9	18.9	31.1	25.6	-	-	-	-	30.0	44.4	59.5	65.5
	SCEN [20]	5.3	18.4	29.9	25.2	2.9	12.4	28.9	12.1	32.0	47.8	63.5	63.1
	CGE [26]	6.5	21.4	32.8	28.0	4.2	15.5	33.5	16.0	33.5	60.5	64.5	71.5
	Co-CGE [24]	6.6	20.0	32.1	28.3	4.1	14.4	33.3	14.9	33.9	48.1	62.3	66.3
	CAPE [15]	6.7	20.4	32.1	28.0	4.6	16.3	33.0	16.4	35.2	49.5	62.3	68.5
With CLIP	CLIP-ZS [33]	11.0	26.1	30.2	46.0	1.4	8.6	7.5	25.0	5.0	15.6	15.8	49.1
	CoOp [49]	13.5	29.8	34.4	47.6	4.4	17.1	26.8	20.5	18.8	34.6	52.1	49.3
	Co-CGE [†] [24]	17.0	33.1	46.7	45.9	5.7	18.9	34.1	21.2	36.3	49.7	63.4	71.3
	CSP [29]	19.4	36.3	46.6	49.9	6.2	20.5	28.8	26.8	33.0	46.6	64.2	66.2
	DFSP [22]	20.6	37.3	46.9	52.0	10.5	27.1	38.2	32.9	36.9	47.2	66.7	71.7
	CAILA (Ours)	23.4	39.9	51.0	53.9	14.8	32.7	43.9	38.5	44.1	57.0	67.8	74.0

Table 2: Quantitative results on generalized CZSL in *closed world*, all numbers are reported in percentage. S and U refer to best seen and unseen accuracy on the accuracy curve. CLIP-ZS refers to the vanilla CLIP model without fine-tuning. All CLIP-based models are run with ViT-L/14 and we conduct extensive experiments in Tab. 4. [†]We run Co-CGE with similar CLIP features and report our best number of the model.

4. Experiments

Here, we present details of experiments: Experimental settings are discussed in Sec. 4.1 and we report quantitative results in Sec. 4.2; we conduct ablation studies in Sec. 4.3.

4.1. Experiment Settings

Datasets. We evaluate CAILA on three popular datasets for CZSL: MIT-States [10], C-GQA [26] and UT-Zappos [45, 46]. MIT-States contains natural objects associated with various fine-grain attributes. Though it is relatively noisy [1] due to the data collection process, it still acts as an effective benchmark for evaluating CZSL models. Derived from GQA [9], C-GQA has a richer set of compositions and a larger vocabulary for attributes and objects, compared with MIT-States. UT-Zappos contains images of shoes with various styles, some of which are even not distinguishable inside the word embedding space. As for splits, we follow [26] for C-GQA, and [32] for MIT-States and UT-Zappos. Statistically, the numbers of images in train/val/test are 30k/10k/10k for MIT-States, 23k/3k/3k for UT-Zappos, and 26k/7k/5k for C-GQA. We also show detailed statistics on individual primitives and compositions in Table. 1.

Scenarios. We perform evaluation of CZSL models on both *closed* and *open* world scenarios and denote them as ● and ○, respectively. Regarding the *closed world* setting, we follow [26, 32, 1] and conduct CZSL with a limited search space. We further run models in the *open* world scenario, proposed by Mancini *et al.* [23], to assess the scalability of CZSL models. It is worth noting that C-GQA becomes much more challenging under the *open world* setting, as the size of the search space drastically increases from 2k to nearly 400k. We also notice similar space expansions on MIT-States, while the number of possible compositions

does not increase much on UT-Zappos.

Evaluation Metrics. Our evaluation is performed under the generalized CZSL protocol adopted by [26, 32, 1, 23]. [32, 42] argue that it is unreasonable to evaluate only Y_u as significant biases enter during training and model selection. They suggest computing both seen and unseen accuracy with various bias values added to unseen categories and taking the Area Under the Curve (AUC) as the core metric. We select our models with the best AUC on validation sets and report their performance on test sets.

Furthermore, best-seen accuracy and best-unseen accuracy are calculated when other candidates are filtered out by specific bias terms. To assess models’ capability of balancing between seen and unseen categories, we also report best *Harmonic Mean* (HM), defined as $(2 * seen * unseen) / (seen + unseen)$.

Implementation Details: We build our model on the PyTorch [30] framework. As for optimization, we use Adam optimizer with a weight decay of $5e - 5$. The learning rate is set to $2e - 5$. The batch size is set to 32 for all three datasets. The temperature τ_C, τ_A, τ_O is set to 0.01, 0.0005 and 0.0005, respectively. Most of the experiments are run on two NVIDIA A100 GPUs. We the number of vision MoA layers M to 6 by default. For the downsampling function f_{Down} , we set the reduction factor to 4. Ablation studies on these settings can be found in Sec 4.3.

4.2. Quantitative Results

In this section, we present quantitative results in detail under both *closed world* and *open world* settings. Such results verify the effectiveness of our method, which surpasses the current SOTA on most metrics, in both scenarios.

Closed World Results. Performance numbers of dif-

	Open World Model	○ MIT-States				○ C-GQA				○ UT-Zappos			
		AUC (↑)	HM (↑)	S (↑)	U (↑)	AUC (↑)	HM (↑)	S (↑)	U (↑)	AUC (↑)	HM (↑)	S (↑)	U (↑)
Without CLIP	CompCos [23]	0.8	5.8	21.4	7.0	0.43	3.3	26.7	2.2	18.5	34.5	53.3	44.6
	CGE [26]	1.0	6.0	32.4	5.1	0.47	2.9	32.7	1.8	23.1	39.0	61.7	47.7
	KG-SP [14]	1.3	7.4	28.4	7.5	0.78	4.7	31.5	2.9	26.5	42.3	61.8	52.1
	Co-CGE ^{CW} [24]	1.1	6.4	31.1	5.8	0.53	3.4	32.1	2.0	23.1	40.3	62.0	44.3
	Co-CGE ^{open} [24]	2.3	10.7	30.3	11.2	0.78	4.8	32.1	3.0	23.3	40.8	61.2	45.8
With CLIP	CLIP-ZS [33]	3.0	12.8	30.1	14.3	0.27	4.0	7.5	4.6	2.2	11.2	15.7	20.6
	CoOp (a)[49]	4.7	16.1	36.8	16.5	0.73	5.7	20.9	4.5	19.5	35.6	61.8	39.3
	CoOp (b)[49]	2.8	12.3	34.6	9.3	0.70	5.5	21.0	4.6	13.2	28.9	52.1	31.5
	Co-CGE [†] [24]	5.6	17.7	38.1	20.0	0.91	5.3	33.2	3.9	28.4	45.3	59.9	56.2
	CSP [29]	5.7	17.4	46.3	15.7	1.20	6.9	28.7	5.2	22.7	38.9	64.1	44.1
	DFSP [22]	6.8	19.3	47.5	18.5	2.40	10.4	38.3	7.2	30.3	44.0	66.8	60.0
	CAILA (Ours)	8.2	21.6	51.0	20.2	3.08	11.5	43.9	8.0	32.8	49.4	67.8	59.7

Table 3: Quantitative results on generalized CZSL in *open world*, all numbers are reported in percentage. S and U refer to best seen and unseen accuracy on the curve. CLIP-ZS refers to the vanilla CLIP model without fine-tuning. All CLIP-based models are run with ViT-L/14. Note that our models tested have identical weights as in Tab. 2. [†]We run Co-CGE with similar CLIP features and report our best number of the model.

Image Encoder	Closed World Model	●MIT-States	●C-GQA	●UT-Zappos
ViT B/32	CLIP-ZS* [33]	7.5	1.2	2.4
	CLIP-FT [33]	10.9	<u>7.6</u>	21.1
	Co-CGE [†] [24]	12.2	5.0	<u>31.2</u>
	CSP* [29]	12.4	5.7	24.2
	DFSP [22]	<u>13.2</u>	-	23.3
	CAILA (Ours)	16.1	10.4	39.0
	Δ	+2.9 (21.9%)	+2.8 (36.8%)	+7.8 (25.0%)
ViT L/14	CLIP-ZS* [33]	11.0	1.4	5.0
	CLIP-FT* [33]	14.4	<u>10.5</u>	4.8
	CoOp* [49]	13.5	4.4	18.8
	CLIP-Adapter* [4]	9.5	3.2	31.5
	Co-CGE [†] [24]	17.0	5.7	36.3
	CSP* [29]	19.4	6.2	33.0
	DFSP [22]	<u>20.6</u>	10.5	36.8
	CAILA (Ours)	23.4	14.8	44.1
	Δ	+2.8 (13.6%)	+4.3 (41.0%)	+7.3 (19.8%)

Table 4: Comparison of the AUC performance on all three benchmarks among CLIP-based models. ZS and FT stand for zero-shot and fine-tuned. Best results are shown in **bold** and runner-ups are underlined. Δ is calculated between CAILA and the second-best. Numbers with * are acquired from the CSP paper [29]. [†]We obtain these numbers by running Co-CGE on similar CLIP features.

ferent models in the *closed world* scenario are reported in Tab. 2. On MIT-States, results show that our model overcomes the label noise and achieves SOTA. More specifically, on the core metric, AUC, we observe a 2.8% improvement, from 20.6% to 23.4%. Furthermore, regarding harmonic mean, CAILA achieves 39.9%, outperforming all baselines. When it comes to best seen and unseen accuracy, our model achieves improvements of $\sim 4\%$ and $\sim 2\%$, respectively.

Adapter		MoA		● MIT-States			
V	L	V	L	AUC (↑)	HM (↑)	S (↑)	U (↑)
CSP [29]				12.4	28.6	36.4	42.5
✓				14.0	30.1	41.4	42.0
	✓			13.9	30.5	40.3	42.8
✓	✓			14.4	30.7	42.2	43.2
✓	✓	✓		15.4	31.4	43.4	44.5
✓	✓		✓	15.2	31.7	41.6	44.8
✓	✓	✓	✓	16.1	32.9	43.3	45.6

Table 5: Ablation on adapters and MoA modules. V and L refer to Vision and Language, respectively.

Our evaluation results on C-GQA further verify the advantage of our proposed mixture module, especially when the number of unseen compositions is larger. On AUC, our model achieves an 4.3% improvement, 40% of the previous SOTA, from 10.5% to 14.8%, even though C-GQA is the hardest among all benchmarks. HM is also improved by 5.6%. Moreover, we observe improvements of 5.7% and 5.6% of best seen and unseen accuracy.

UT-Zappos has much fewer attributes and object categories, compared with its counterparts, and is thus much easier, as the gap between various methods is smaller. But it is noticeable that our model, CAILA, outperforms all other baselines, with an 7.2% improvement on the AUC metric.

Open World Results. We further conduct experiments under the *open world* setting to evaluate the robustness of our model. Results are shown in Tab. 3. Noticeably, the *open world* scenario is much harder than the *closed world*, as performance on all benchmarks drops drastically, while CAILA achieves SOTA on most metrics in this scenario without any composition filtering techniques adopted in the previous papers [23, 24, 29].

Adapter and MoA. We evaluate different adapter/MoA

Closed World Model	Mixture		● MIT-States			
	\mathbf{z}	\mathbf{h}'	AUC (\uparrow)	HM (\uparrow)	S (\uparrow)	U (\uparrow)
	✓	✓	16.1	32.9	43.3	45.6
CAILA (Ours)	✓		15.8	32.2	43.3	45.2
			15.5	31.7	43.0	45.1
		✓	15.5	32.0	42.7	44.8

Table 6: Ablation on vision MoA strategies.

Closed World Model	● MIT-States			
	AUC (\uparrow)	HM (\uparrow)	S (\uparrow)	U (\uparrow)
CAILA(Ours)	16.1	32.9	43.3	45.6
w/o Learnable Prompts	15.8	32.1	43.5	44.6
DFSP [22]	13.2	29.4	36.7	43.4
CSP [29]	12.4	28.6	36.4	42.5

Table 7: Ablation study on learnable prompts.

settings on MIT-States and report results in Tab. 5. We observe that compared with CSP [29], adding adapters to either side of encoders can effectively improve the performance while attaching adapters to both sides shows further improvements. Experiments in the last three rows verify that our Mixture-of-Adapters mechanism further improves the performance when it is applied on both sides.

On MIT-States, our approach greatly outperforms SOTA on all metrics, particularly the AUC. Our model brings up AUC from 6.8% to 8.2%, while achieving a 21.6% harmonic mean, 2.3% higher than the previous SOTA. Moreover, CAILA achieves improves seen object accuracy by 3.5% and unseen object accuracy by 0.2%.

The performance of CAILA on C-GQA in the *open world* scenario is consistent with the one in *closed world*, indicating that our model performs well under both settings, especially on the hardest benchmark. More specifically, our model achieves 3.08% AUC, 128% of DFSP [22]. We also observe a $\sim 10\%$ relative improvement on harmonic mean, from 10.4% to 11.5%. CAILA achieves 5.6% and 0.8% improvements on seen and unseen accuracy respectively.

Regarding UT-Zappos, which merely has less than 110 compositions in *open world*, our model also brings in performance gains. It achieves a 49.4% harmonic mean, 4.1% higher than Co-CGE. CAILA also gets the best AUC of 32.8%, at least 2% higher against other baselines.

Comparisons between CLIP-based methods. We further make head-to-head comparisons between CAILA and other approaches built with CLIP in Tab. 4, with variations on the vision encoder: ViT-B/32 [3] and ViT-L/14. Results verify CAILA’s effectiveness and consistency with different visual backbones. In particular, CAILA achieves $>35\%$ relative improvements on C-GQA against other baselines, regardless of the vision encoder. It is also worth noting that CAILA, a partially fine-tuned model, performs much

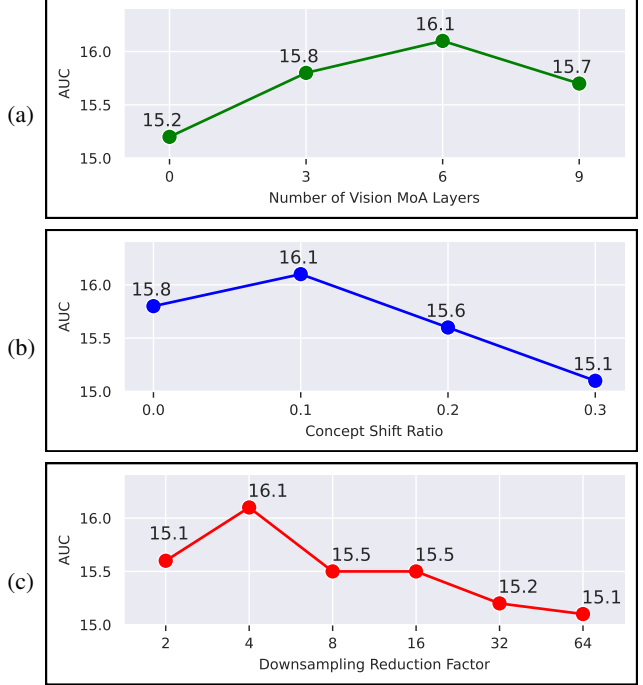


Figure 5: Ablation studies on CAILA setups: (a) The number of vision MoA layer M ; (b) The ratio of concept shift during training; (c) The reduction factor of f_{Down} .

better than the fully fine-tuned CLIP model, indicating that CAILA better suppresses training biases while remaining sharp on knowledge transfer for CZSL. In addition, we notice that the fully fine-tuned CLIP with ViT L/14 fails on UT-Zappos while the one with ViT B/32 yields reasonable performance. We attribute the failure to the size difference between ViT L/14 and the dataset, as ViT-Large has a large number of parameters while UT-Zappos has fewer samples and categories, compared with other benchmarks.

4.3. Ablation Studies

In this section, we perform ablation studies to present CAILA in depth. Due to the restraints of computing resources, all experiments in this section are conducted with CLIP ViT-B/32 and MIT-States in *closed world*.

Vision Mixture Strategy. We compare different ways of mixing \mathbf{z} and \mathbf{h}' inside the vision MoA layer as described in Eqn. 4.5. Tab. 6 shows the results of mixing only one of the feature vectors or none at all. The last row corresponds to averaging $\mathcal{F}_A(x)$, $\mathcal{F}_O(x)$, $\mathcal{F}_C(x)$ without intra-layer mixture, which is similar to the language side MoA. Experiment results demonstrate that mixing both \mathbf{z} and \mathbf{h}' as proposed in Sec. 3.3 yields optimal performance while applying a similar strategy as the language side hurts.

Learnable Prompts. We perform experiments to study the effect of learnable prompts in our framework. Results

reported in Tab. 7 show that our model remains competitive with prompt embeddings fixed. Such behavior justifies that performance gains of CAILA come from designs that have been discussed in the Approach section.

CAILA Setups. We explore different aspects of our setup and show the results in Fig. 5. Fig. 5(a) demonstrates that CAILA performs better with MoA layers and achieves the best performance with 6 MoA layers on the vision side; Fig. 5(b) indicates that replacing 10% of a batch with post-shift features can increase the AUC while adding more shift reduces it; In Fig. 5(c), we find that the optimal reduction factor for the latent feature z is 4, while using higher reduction factors does not affect the performance significantly and can be considered for efficiency reasons.

5. Conclusion

In this paper, we explore the problem of how to leverage large-scale Vision-Language Pre-trained (VLP) models, particularly CLIP, more effectively for compositional zero-shot learning. Unlike previous methods which treat CLIP as a black box, we propose to slightly modify the architecture and attach Concept-Aware Intra-Layer Adapters (CAILA) to each layer of the CLIP encoder to enhance the knowledge transfer from CLIP to CZSL. Moreover, we design the mixture-of-adapters mechanism to further improve the generalizability of the model. Quantitative evaluations demonstrate that CAILA achieves significant improvements on all three common benchmarks. We also provide comprehensive discussions on deciding the optimal setup.

References

- [1] Yuval Atzmon, Felix Kreuk, Uri Shalit, and Gal Chechik. A causal view of compositional zero-shot recognition. *arXiv preprint arXiv:2006.14610*, 2020.
- [2] Shiming Chen, Wenjie Wang, Beihao Xia, Qinmu Peng, Xinge You, Feng Zheng, and Ling Shao. Free: Feature refinement for generalized zero-shot learning. In *Proceedings of the IEEE/CVF International Conference on Computer Vision*, pages 122–131, 2021.
- [3] Alexey Dosovitskiy, Lucas Beyer, Alexander Kolesnikov, Dirk Weissenborn, Xiaohua Zhai, Thomas Unterthiner, Mostafa Dehghani, Matthias Minderer, Georg Heigold, Sylvain Gelly, Jakob Uszkoreit, and Neil Houlsby. An image is worth 16x16 words: Transformers for image recognition at scale. In *International Conference on Learning Representations*, 2021.
- [4] Peng Gao, Shijie Geng, Renrui Zhang, Teli Ma, Rongyao Fang, Yongfeng Zhang, Hongsheng Li, and Yu Qiao. Clip-adapter: Better vision-language models with feature adapters. *arXiv preprint arXiv:2110.04544*, 2021.
- [5] Sonam Goenka, Zhaoheng Zheng, Ayush Jaiswal, Rakesh Chada, Yue Wu, Varsha Hedau, and Pradeep Natarajan. Fashionvlp: Vision language transformer for fashion retrieval with feedback. In *Proceedings of the IEEE/CVF Conference on Computer Vision and Pattern Recognition*, pages 14105–14115, 2022.
- [6] Kaiming He, Xiangyu Zhang, Shaoqing Ren, and Jian Sun. Deep residual learning for image recognition. In *Proceedings of the IEEE conference on computer vision and pattern recognition*, pages 770–778, 2016.
- [7] Neil Houlsby, Andrei Giurgiu, Stanislaw Jastrzebski, Bruna Morrone, Quentin De Laroussilhe, Andrea Gesmundo, Mona Attariyan, and Sylvain Gelly. Parameter-efficient transfer learning for nlp. In *International Conference on Machine Learning*, pages 2790–2799. PMLR, 2019.
- [8] Xiaowei Hu, Zhe Gan, Jianfeng Wang, Zhengyuan Yang, Zicheng Liu, Yumao Lu, and Lijuan Wang. Scaling up vision-language pre-training for image captioning. In *Proceedings of the IEEE/CVF Conference on Computer Vision and Pattern Recognition*, pages 17980–17989, 2022.
- [9] Drew A Hudson and Christopher D Manning. Gqa: A new dataset for real-world visual reasoning and compositional question answering. In *Proceedings of the IEEE/CVF conference on computer vision and pattern recognition*, pages 6700–6709, 2019.
- [10] Phillip Isola, Joseph J Lim, and Edward H Adelson. Discovering states and transformations in image collections. In *Proceedings of the IEEE conference on computer vision and pattern recognition*, pages 1383–1391, 2015.
- [11] Chao Jia, Yinfei Yang, Ye Xia, Yi-Ting Chen, Zarana Parekh, Hieu Pham, Quoc Le, Yun-Hsuan Sung, Zhen Li, and Tom Duerig. Scaling up visual and vision-language representation learning with noisy text supervision. In *International Conference on Machine Learning*, pages 4904–4916. PMLR, 2021.
- [12] Michael Kampffmeyer, Yinbo Chen, Xiaodan Liang, Hao Wang, Yujia Zhang, and Eric P Xing. Rethinking knowledge graph propagation for zero-shot learning. In *Proceedings of the IEEE/CVF Conference on Computer Vision and Pattern Recognition*, pages 11487–11496, 2019.
- [13] Rabeeh Karimi Mahabadi, James Henderson, and Sebastian Ruder. Compacter: Efficient low-rank hypercomplex adapter layers. *Advances in Neural Information Processing Systems*, 34:1022–1035, 2021.
- [14] Shyamgopal Karthik, Massimiliano Mancini, and Zeynep Akata. Kg-sp: Knowledge guided simple primitives for open world compositional zero-shot learning. In *Proceedings of the IEEE/CVF Conference on Computer Vision and Pattern Recognition*, pages 9336–9345, 2022.
- [15] Muhammad Gul Zain Ali Khan, Muhammad Ferjad Naeem, Luc Van Gool, Alain Pagani, Didier Stricker, and Muhammad Zeshan Afzal. Learning attention propagation for compositional zero-shot learning. In *Proceedings of the IEEE/CVF Winter Conference on Applications of Computer Vision*, pages 3828–3837, 2023.
- [16] Thomas N. Kipf and Max Welling. Semi-supervised classification with graph convolutional networks. In *5th International Conference on Learning Representations, ICLR 2017, Toulon, France, April 24–26, 2017, Conference Track Proceedings*. OpenReview.net, 2017.
- [17] Christoph H Lampert, Hannes Nickisch, and Stefan Harmeling. Attribute-based classification for zero-shot visual object

- categorization. *IEEE transactions on pattern analysis and machine intelligence*, 36(3):453–465, 2013.
- [18] Brian Lester, Rami Al-Rfou, and Noah Constant. The power of scale for parameter-efficient prompt tuning. *arXiv preprint arXiv:2104.08691*, 2021.
 - [19] Junnan Li, Ramprasaath Selvaraju, Akhilesh Gotmare, Shafiq Joty, Caiming Xiong, and Steven Chu Hong Hoi. Align before fuse: Vision and language representation learning with momentum distillation. *Advances in neural information processing systems*, 34:9694–9705, 2021.
 - [20] Xiangyu Li, Xu Yang, Kun Wei, Cheng Deng, and Muli Yang. Siamese contrastive embedding network for compositional zero-shot learning. In *Proceedings of the IEEE/CVF Conference on Computer Vision and Pattern Recognition*, pages 9326–9335, 2022.
 - [21] Yong-Lu Li, Yue Xu, Xiaohan Mao, and Cewu Lu. Symmetry and group in attribute-object compositions. In *Proceedings of the IEEE/CVF Conference on Computer Vision and Pattern Recognition*, pages 11316–11325, 2020.
 - [22] Xiaocheng Lu, Song Guo, Ziming Liu, and Jingcai Guo. Decomposed soft prompt guided fusion enhancing for compositional zero-shot learning. In *Proceedings of the IEEE/CVF Conference on Computer Vision and Pattern Recognition*, pages 23560–23569, 2023.
 - [23] Massimiliano Mancini, Muhammad Ferjad Naeem, Yongqin Xian, and Zeynep Akata. Open world compositional zero-shot learning. In *Proceedings of the IEEE/CVF Conference on Computer Vision and Pattern Recognition*, pages 5222–5230, 2021.
 - [24] Massimiliano Mancini, Muhammad Ferjad Naeem, Yongqin Xian, and Zeynep Akata. Learning graph embeddings for open world compositional zero-shot learning. *IEEE Transactions on Pattern Analysis and Machine Intelligence*, 2022.
 - [25] Ishan Misra, Abhinav Gupta, and Martial Hebert. From red wine to red tomato: Composition with context. In *Proceedings of the IEEE Conference on Computer Vision and Pattern Recognition*, pages 1792–1801, 2017.
 - [26] Muhammad Ferjad Naeem, Yongqin Xian, Federico Tombari, and Zeynep Akata. Learning graph embeddings for compositional zero-shot learning. In *Proceedings of the IEEE/CVF Conference on Computer Vision and Pattern Recognition*, pages 953–962, 2021.
 - [27] Tushar Nagarajan and Kristen Grauman. Attributes as operators: factorizing unseen attribute-object compositions. In *Proceedings of the European Conference on Computer Vision (ECCV)*, pages 169–185, 2018.
 - [28] Zhixiong Nan, Yang Liu, Nanning Zheng, and Song-Chun Zhu. Recognizing unseen attribute-object pair with generative model. In *Proceedings of the AAAI Conference on Artificial Intelligence*, volume 33, pages 8811–8818, 2019.
 - [29] Nihal V. Nayak, Peilin Yu, and Stephen Bach. Learning to compose soft prompts for compositional zero-shot learning. In *International Conference on Learning Representations*, 2023.
 - [30] Adam Paszke, Sam Gross, Francisco Massa, Adam Lerer, James Bradbury, Gregory Chanan, Trevor Killeen, Zeming Lin, Natalia Gimelshein, Luca Antiga, et al. Pytorch: An imperative style, high-performance deep learning library. *Advances in neural information processing systems*, 32:8026–8037, 2019.
 - [31] Jeffrey Pennington, Richard Socher, and Christopher D Manning. Glove: Global vectors for word representation. In *Proceedings of the 2014 conference on empirical methods in natural language processing (EMNLP)*, pages 1532–1543, 2014.
 - [32] Senthil Purushwalkam, Maximilian Nickel, Abhinav Gupta, and Marc’Aurelio Ranzato. Task-driven modular networks for zero-shot compositional learning. In *Proceedings of the IEEE/CVF International Conference on Computer Vision*, pages 3593–3602, 2019.
 - [33] Alec Radford, Jong Wook Kim, Chris Hallacy, Aditya Ramesh, Gabriel Goh, Sandhini Agarwal, Girish Sastry, Amanda Askell, Pamela Mishkin, Jack Clark, et al. Learning transferable visual models from natural language supervision. In *International Conference on Machine Learning*, pages 8748–8763. PMLR, 2021.
 - [34] Scott Reed, Zeynep Akata, Honglak Lee, and Bernt Schiele. Learning deep representations of fine-grained visual descriptions. In *Proceedings of the IEEE conference on computer vision and pattern recognition*, pages 49–58, 2016.
 - [35] Frank Ruis, Gertjan Burghouts, and Doina Bucur. Independent prototype propagation for zero-shot compositional-ity. *Advances in Neural Information Processing Systems*, 34, 2021.
 - [36] Nirat Saini, Khoi Pham, and Abhinav Shrivastava. Disentangling visual embeddings for attributes and objects. In *Proceedings of the IEEE/CVF Conference on Computer Vision and Pattern Recognition*, pages 13658–13667, 2022.
 - [37] Richard Socher, Milind Ganjoo, Hamsa Sridhar, Osbert Bastani, Christopher D Manning, and Andrew Y Ng. Zero-shot learning through cross-modal transfer. *arXiv preprint arXiv:1301.3666*, 2013.
 - [38] Yi-Lin Sung, Jaemin Cho, and Mohit Bansal. VI-adapter: Parameter-efficient transfer learning for vision-and-language tasks. In *Proceedings of the IEEE/CVF Conference on Computer Vision and Pattern Recognition*, pages 5227–5237, 2022.
 - [39] Xiaolong Wang, Yufei Ye, and Abhinav Gupta. Zero-shot recognition via semantic embeddings and knowledge graphs. In *Proceedings of the IEEE conference on computer vision and pattern recognition*, pages 6857–6866, 2018.
 - [40] Xin Wang, Fisher Yu, Ruth Wang, Trevor Darrell, and Joseph E Gonzalez. Tafe-net: Task-aware feature embeddings for low shot learning. In *Proceedings of the IEEE/CVF Conference on Computer Vision and Pattern Recognition*, pages 1831–1840, 2019.
 - [41] Kun Wei, Muli Yang, Hao Wang, Cheng Deng, and Xianglong Liu. Adversarial fine-grained composition learning for unseen attribute-object recognition. In *Proceedings of the IEEE/CVF International Conference on Computer Vision*, pages 3741–3749, 2019.
 - [42] Yongqin Xian, Christoph H Lampert, Bernt Schiele, and Zeynep Akata. Zero-shot learning—a comprehensive evaluation of the good, the bad and the ugly. *IEEE transactions*

on pattern analysis and machine intelligence, 41(9):2251–2265, 2018.

- [43] Yongqin Xian, Tobias Lorenz, Bernt Schiele, and Zeynep Akata. Feature generating networks for zero-shot learning. In *Proceedings of the IEEE conference on computer vision and pattern recognition*, pages 5542–5551, 2018.
- [44] Muli Yang, Cheng Deng, Junchi Yan, Xianglong Liu, and Dacheng Tao. Learning unseen concepts via hierarchical decomposition and composition. In *Proceedings of the IEEE/CVF Conference on Computer Vision and Pattern Recognition*, pages 10248–10256, 2020.
- [45] A. Yu and K. Grauman. Fine-grained visual comparisons with local learning. In *Computer Vision and Pattern Recognition (CVPR)*, Jun 2014.
- [46] A. Yu and K. Grauman. Semantic jitter: Dense supervision for visual comparisons via synthetic images. In *International Conference on Computer Vision (ICCV)*, Oct 2017.
- [47] Li Zhang, Tao Xiang, and Shaogang Gong. Learning a deep embedding model for zero-shot learning. In *Proceedings of the IEEE conference on computer vision and pattern recognition*, pages 2021–2030, 2017.
- [48] Kaiyang Zhou, Jingkang Yang, Chen Change Loy, and Ziwei Liu. Conditional prompt learning for vision-language models. In *Proceedings of the IEEE/CVF Conference on Computer Vision and Pattern Recognition*, pages 16816–16825, 2022.
- [49] Kaiyang Zhou, Jingkang Yang, Chen Change Loy, and Ziwei Liu. Learning to prompt for vision-language models. *International Journal of Computer Vision*, 130(9):2337–2348, 2022.
- [50] Yizhe Zhu, Mohamed Elhoseiny, Bingchen Liu, Xi Peng, and Ahmed Elgammal. A generative adversarial approach for zero-shot learning from noisy texts. In *Proceedings of the IEEE conference on computer vision and pattern recognition*, pages 1004–1013, 2018.